

Surface-Mediated Hydrogen Bonding of Proteinogenic α -Amino Acids on Silicon

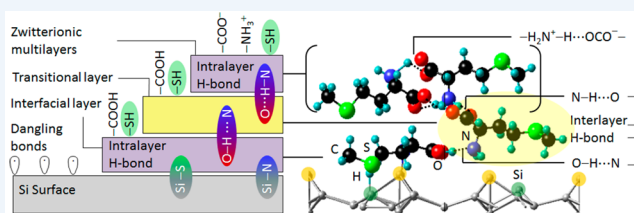
Fatemeh R. Rahsepar, Nafiseh Moghimi, and K. T. Leung*

WATLab and Department of Chemistry, University of Waterloo, Waterloo, Ontario N2L 3G1, Canada

S Supporting Information

CONSPECTUS: Understanding the adsorption, film growth mechanisms, and hydrogen bonding interactions of biological molecules on semiconductor surfaces has attracted much recent attention because of their applications in biosensors, biocompatible materials, and biomolecule-based electronic devices. One of the most challenging questions when studying the behavior of biomolecules on a metal or semiconductor surface is “What are the driving forces and film growth mechanisms for biomolecular adsorption on these surfaces?” Despite a large volume of work on self-assembly of amino acids on single-crystal metal surfaces, semiconductor surfaces offer more direct surface-mediated interactions and processes with biomolecules. This is due to their directional surface dangling bonds that could significantly perturb hydrogen bonding arrangements.

For all the proteinogenic biomolecules studied to date, our group has observed that they generally follow a “universal” three-stage growth process on Si(111)7 \times 7 surface. This is supported by corroborating data obtained from a three-pronged approach of combining chemical-state information provided by X-ray photoelectron spectroscopy (XPS) and the site-specific local density-of-state images obtained by scanning tunneling microscopy (STM) with large-scale quantum mechanical modeling based on the density functional theory with van der Waals corrections (DFT-D2). Indeed, this three-stage growth process on the 7 \times 7 surface has been observed for small benchmark biomolecules, including glycine (the simplest nonchiral amino acid), alanine (the simplest chiral amino acid), cysteine (the smallest amino acid with a thiol group), and glycyglycine (the smallest (di)peptide of glycine). Its universality is further validated here for the other sulfur-containing proteinogenic amino acid, methionine. We use methionine as an example of prototypical proteinogenic amino acids to illustrate this surface-mediated process. This type of growth begins with the formation of a covalent-bond driven interfacial layer (first adlayer), followed by that of a transitional layer driven by interlayer and intralayer hydrogen bonding (second adlayer), and then finally the zwitterionic multilayers (with intralayer hydrogen bonding). The important role of surface-mediated hydrogen bonding as the key for this universal three-stage growth process is demonstrated. This finding provides new insight into biomolecule–semiconductor surface interactions often found in biosensors and biomolecular electronic devices. We also establish the trends in the H-bond length among different types of the hydrogen bonding for dimolecular structures in the gas phase and on the Si(111)7 \times 7 surface, the latter of which could be validated by their STM images. Finally, five simple rules of thumb are developed to summarize the adsorption properties of these proteinogenic biomolecules as mediated by hydrogen bonding, and they are expected to provide a helpful guide to future studies of larger biomolecules and their potential applications.



■ INTRODUCTION

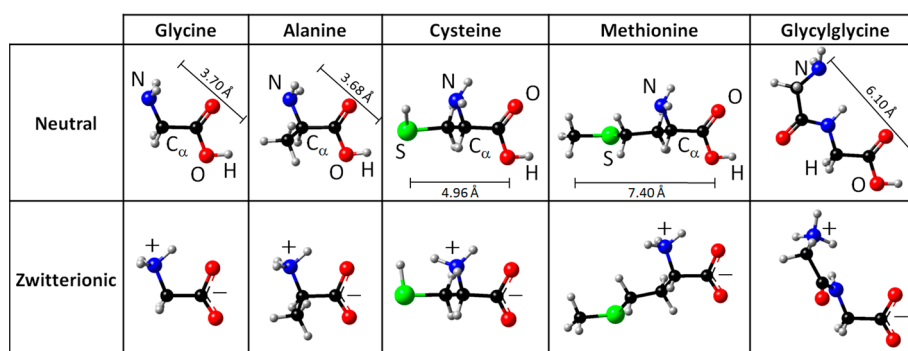
Molecular interactions of biomaterials with semiconductor surfaces have attracted much recent attention because of their applications in biosensors, biocompatible materials, and biomolecule-based electronic devices.^{1–4} Among the most fundamental biomolecules, amino acids and nucleotides are the basic building blocks of larger biological materials such as proteins, peptides, and DNAs. One of the most challenging questions when studying the adsorption behavior of amino acids on a metal or semiconductor surface is “What are the driving forces and film growth mechanisms for their adsorption on these surfaces?” Despite the large number of studies of adsorbed amino acids on various surfaces of single-crystal metals,^{5–32} only a few investigations of their adsorption on semiconductor surfaces^{33–36} have been reported. A major

impetus behind the research in biological surface chemistry of semiconductors is their potential to convert biological information directly into electrical signals. Unlike the long-range, noncovalent interactions between adsorbed amino acids and metal surfaces, the availability of directional dangling bonds on semiconductor surfaces makes feasible direct covalent bonding with biomolecules, thus providing the opportunity to create a highly stable, multifunctional interface through surface-mediated hydrogen bonding.^{33–36} The lack of covalent bonding between bio-organic molecules and a single-crystal metal surface often leads to self-assembly of these bio-organic molecules purely driven by hydrogen bonding.^{15,25,30,37–39}

Received: December 9, 2015

Published: March 25, 2016

Scheme 1. Ball-and-Stick Models of Neutral and Zwitterionic Equilibrium Structures of Isolated Aliphatic Proteinogenic Biomolecules: Glycine, D-Alanine, L-Cysteine, L-Methionine, and Glycylglycine^a



^aThese structures are generated by DFT-D2 calculations and the molecular lengths (i.e., the separation between the hydroxyl O atom and the farthest non-H atom along the carbon chain backbone) are shown in angstrom (Å). No change in the molecular length of the zwitterionic structure from that of the neutral structure is found for all biomolecules, except for methionine with a 3% increase.

Furthermore, interactions of amino acids with metal surfaces lead to generally weak zwitterionic forms or to binding through both amino and carboxylic acid groups in anionic state, which consumes all the free functional groups and therefore leaves little prospect for building a stable biological interface.

Among all semiconductors, the 7×7 reconstruction of the Si(111) surface offers a variety of interesting reaction sites, with several different site-to-site separations specific for individual bio-organic molecules. These sites allow exploration of the reactivity and selectivity of site-specific processes especially for amino acids containing multiple functional groups. In addition to covalent bonding with the dangling bonds of Si adatom sites, amino acids also offer novel hydrogen bonding among themselves due to the amino and carboxylic acid groups. Hydrogen bonding, both intralayer and interlayer, introduces new film growth and biofunctionalization mechanisms. Quantitative studies of hydrogen bonding interactions are therefore essential for understanding of not only formation of isolated molecular clusters in the gas phase but also important biological processes in physicochemical terms, including self-assembly of supramolecular nanostructures on the surface.³⁷

We observe a “universal” three-stage growth process on the 7×7 surface for small benchmark biomolecules studied to date, including glycine (the simplest nonchiral amino acid), alanine (the simplest chiral amino acid), cysteine (the smallest amino acid with a thiol group), and glycylglycine (a dipeptide of glycine). Its universality is further validated here for the other sulfur-containing proteinogenic amino acid, methionine. Scheme 1 shows the equilibrium geometries of the neutral and zwitterionic forms of the five benchmark proteinogenic biomolecules, which are obtained by DFT-D2 calculations. In our earlier study of glycine on Si(111)7×7,³⁴ we observed the existence of a transitional layer between the interfacial layer and zwitterionic layer for the first time. In our follow-up study of glycylglycine on the 7×7 surface,³⁵ we proposed a growth model involving sequential formation of the covalently bonded interfacial layer, the hydrogen-bond mediated transitional layer, and zwitterionic multilayers. In our recent work on cysteine on Si(111)7×7,³³ we again observed a three-stage growth process, from chemisorbed interfacial layer (first stage) to transitional layer (second stage) and to zwitterionic multilayer film (third stage). This growth sequence is a direct consequence of surface-mediated hydrogen bonding. Using methionine as a typical example, we provide X-ray photoelectron spectroscopy

(XPS) analysis and follow the chemical-state evolution of this three-stage nanofilm growth process from submonolayer to multilayers on Si(111)7×7 and the subsequent thermal evolution. Here, we also employ DFT-D2^{40–49} calculations to investigate the role of hydrogen bonding in the formation of dimolecular configurations of these five benchmark proteinogenic biomolecules first in the gas phase and then on the 7×7 surface. We then show that these surface-mediated hydrogen bonds provide the key to the universal three-stage growth process. This finding provides new insight into biomolecule–semiconductor surface interactions often found in biosensor and biomolecular electronic devices.^{1–4}

■ HYDROGEN BONDING IN PROTEINOGENIC BIOMOLECULES IN THE GAS PHASE

Hydrogen bonding represents the most important type of interaction in the formation of proteins and larger biological materials from the amino acid building blocks. We show, in Figure 1, the dimolecular equilibrium structures resulting from formation of various H-bonds between different functional groups of the aforementioned “isolated” proteinogenic biomolecules (i.e., in the gas phase) obtained by DFT-D2 calculations. The presence of two terminal functional groups, amino and carboxylic acid groups, in glycine, alanine, and methionine could lead to the formation of four types of single H-bonds (O–H···N, O–H···O, N–H···N, N–H···O) and two types of double H-bond configurations [2 × (O–H···O), 2 × (N–H···O)]. The H-bond configurations in the dipeptide of glycine (glycylglycine) are similar to those in glycine, except for the missing double N–H···O H-bond configuration due to the steric hindrance effect. Furthermore, L-cysteine is a good representative of α-amino acids with the added functionality of a thiol (–SH) group in the side chain to serve as an H-bond donor or acceptor. The thiol group gives rise to four additional types of single H-bonds (O–H···S, S–H···O, N–H···S, S–H···S) and one more type of double H-bond configurations [2 × (S–H···N)]. Among the single H-bond configurations, the O–H···N bond is the strongest, which is in good accord with what makes the amino acid molecules the basic building blocks in biomolecular systems. The H-bond lengths in dimolecular configurations of isolated α-amino acids in the gas phase follow the ascending trend O–H···N < O–H···O < N–H···N < N–H···O. When the side-chain –SH H-bond donor or acceptor in

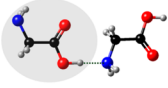
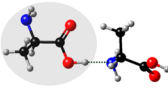
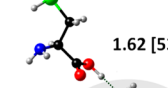
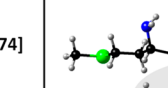
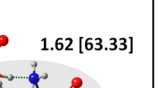
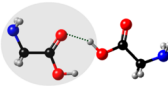
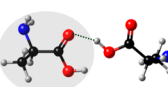
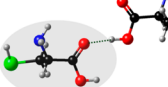
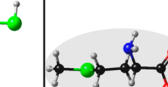
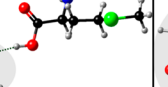
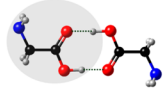
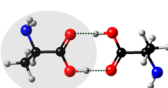
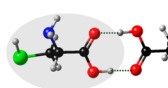
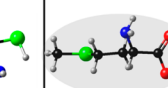
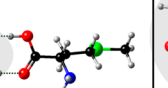
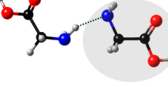
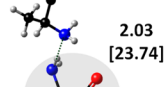
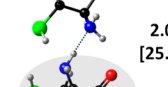

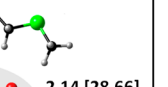
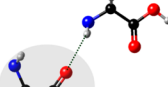
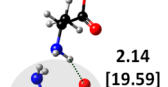
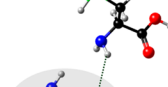
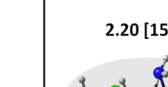
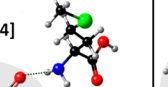
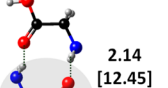
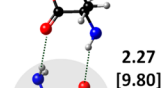
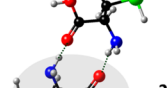
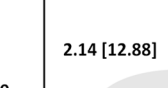
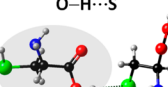
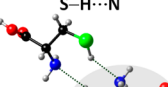
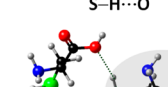
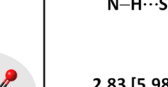
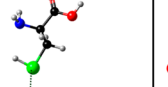
H-Bond Bond Length (Å) [Bond Energy (kJ/mol)]	Glycine	Alanine	Cysteine	Methionine	Glycylglycine
O–H...N	 1.66 [59.44]	 1.65 [59.44]	 1.62 [53.74]	 1.62 [63.33]	 1.69 [53.55]
O–H...O	 1.75 [40.24]	 1.74 [40.52]	 1.73 [29.04]	 1.74 [30.20]	 1.70 [33.09]
O–H...O O–H...O	 1.56 [42.07]	 1.56 [42.55]	 1.56 [40.91]	 1.56 [42.31]	 1.55 [41.78]
N–H...N	 2.12 [22.29]	 2.03 [23.74]	 2.00 [25.57]	 2.14 [28.66]	 2.27 [23.16]
N–H...O	 2.55 [10.3]	 2.14 [19.59]	 2.31 [9.26]	 2.20 [15.24]	 2.16 [20.45]
N–H...O N–H...O	 2.14 [12.45]	 2.27 [9.80]	 2.30 [9.94]	 2.14 [12.88]	
Cysteine	 2.17 [34.93]	 2.35 [7.51]	 2.27 [6.75]	 2.83 [5.98]	 2.84 [5.60]

Figure 1. DFT-D2 calculations of dimolecular structures in the gas phase. Dimolecular structures result from formation of various types of H-bonds (marked by dashed lines) between different functional groups of isolated biomolecules. The calculated bond length (in Å) is depicted along with the corresponding bond energy (in kJ/mol) shown in square parentheses. The molecule in the gray oval is shown with the >C–COOH group in plane in order to provide a reference orientation for the H-bond. The bottom row shows additional –SH donor or acceptor H-bonds in dimolecular configurations of cysteine.

cysteine is included, the corresponding trend for the H-bond lengths becomes O–H...S (< S–H...O) < N–H...S ≈ S–H...S.

It is clear that the O–H group is a stronger H-bond donor than the N–H group, with the S–H group being the weakest. The structures shown in Figure 1 therefore provide useful reference to the type of plausible hydrogen bonding formation and their approximate bond strengths for other amino acids, peptides, and proteins in the gas phase. The general trends in

H-bond strengths obtained above also offer insight into H-bond formation on surfaces.

■ HYDROGEN BONDING IN PROTEINOGENIC NANOFILM GROWTH ON Si(111)7×7

On the surface, dimolecule formation is affected not just by hydrogen bonding but also by surface chemical bonding used

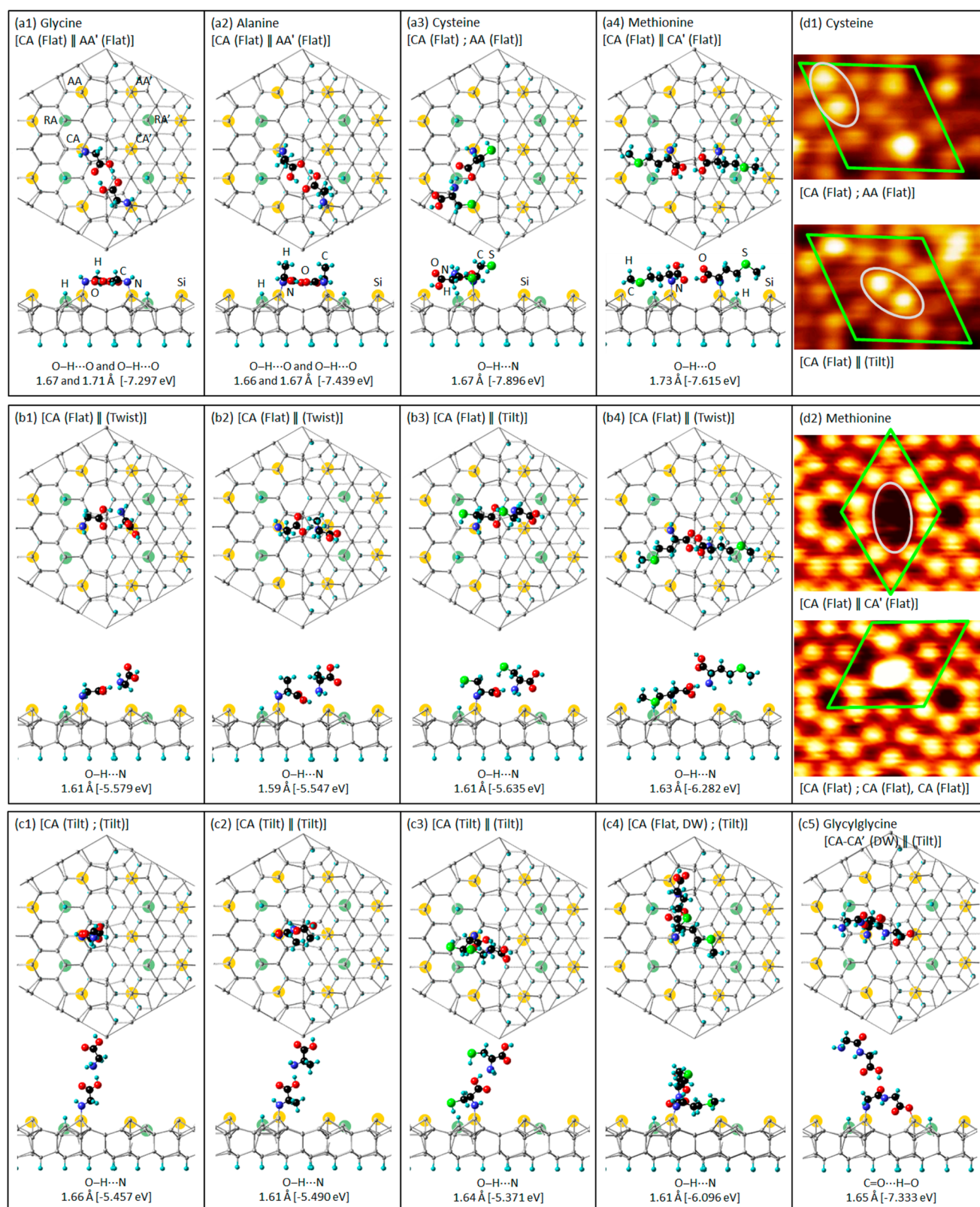


Figure 2. DFT-D2 calculations of dimolecular structures on Si(111)7×7. Top and side views of the most stable adsorption configurations for two proteinogenic biomolecules connected by (a1–a4) flat configurations with intralayer H-bond in the interfacial layer, (b1–b4) lateral configurations and (c1–c5) near-vertical configurations with interlayer H-bond in the transitional layer on a Si₂₀₀H₄₉ model 7×7 surface, as obtained by DFT-D2 calculations. The lengths (in Å) of the respective H-bonds are indicated, along with the corresponding bond energies (in eV) shown in square brackets. The biomolecules are (a1,b1,c1) glycine, (a2,b2,c2) alanine, (a3,b3,c3) cysteine, (a4,b4,c4) methionine, and (c5) glycylglycine. For clarity, the Si adatoms [corner adatom (AA) and center adatom (CA)] and restatoms (RA) are highlighted by larger yellow and green circles, respectively. The Si unit cell is shown cropped in order to provide a higher magnification of the adsorption region. A prime symbol is used to denote a substrate atom in the adjacent half unit cell. Each panel heading denotes the orientation of the >C–COOH backbone in the admolecules with respect to Si

Figure 2. continued

surface (as flat, tilt, or twist) at specific Si adatom sites, with the double bar (||) and semicolon (;) indicating the second molecule H-bonded, respectively, across the dimer wall and within the same half unit cell. (d1) STM empty-state images of cysteine: (upper image) flat dimolecular structure within a half unit cell (a3) and (lower image) tilted dimolecular structure across the dimer wall (b3). (d2) STM empty-state images of methionine: (upper image) flat dimolecular structure across the dimer wall (a4) and (lower image) trimolecular structure within a half unit cell. The STM empty-state images of cysteine and methionine are obtained with a sample bias of +2 V and of +1.7 V, respectively, and a tunneling current of 200 pA.

for anchoring the adsorbate to the surface through a preferred functional group. This type of molecular self-organization is also influenced by steric hindrance on the adsorbate as imposed by the surface atoms and other adsorbates and by the available physical separations between specific adatom sites on the 7×7 surface (Supporting Information, section 1). These constraints eliminate many of the gas-phase H-bonded dimolecular structures shown in Figure 1.

The equilibrium H-bonded dimolecular structures of proteinogenic biomolecules on the Si₂₀₀H₄₉ model surface can be categorized as either “flat” configurations for intralayer H-bonds in the interfacial layer (first adlayer) or “lateral”/“near-vertical” configurations for interlayer H-bonds in the formation of the transitional layer or second adlayer (Supporting Information, Table S1). Among all of these, dimolecular flat configurations (containing intralayer hydrogen bonding) that are covalently bonded to the Si adatoms through the dehydrogenated amino group, the cyclic dimolecular structures with double O–H···O H-bonds across the dimer wall (Figure 2a1,a2), single O–H···O H-bond across the dimer wall (Figure 2a4), and single O–H···N H-bond within a half unit cell (Figure 2a3) are found to be the most stable in the interfacial layer. On the other hand, both lateral (Figure 2b1–b4) and near-vertical (Figure 2c1–c4) configurations of all proteinogenic biomolecules except glycylglycine involving interlayer O–H···N H-bond are the most stable structures in the transitional layer. For the near-vertical configurations (Supporting Information, sections 2 and 3), the O–H···N H-bond length is shorter than the N–H···O H-bond length, which is in good accord with the trends found for dimolecule systems in the gas phase (Figure 1). For both glycine and alanine, our calculations show that the cyclic double O–H···O hydrogen bonding provides the most stable interfacial bonding for the flat arrangements on the Si surface (Figure 2a1,a2), while the O–H···N hydrogen bonding provides the best lateral (Figure 2b1,b2) and near-vertical configurations (Figure 2c1,c2) for forming the transitional layer. These configurations are supported by our XPS results.^{33–36} Our DFT-D2 calculations also show that the configuration with the lateral O–H···N H-bond (Figure 2a3) is only slightly more stable (by 0.015 eV) than that of the double O–H···O H-bonds in cysteine (Supporting Information, section 3), in contrast to other amino acids. For the other S-containing α -amino acid, methionine, the most stable configurations with flat and lateral/near-vertical hydrogen bonding are the single O–H···O H-bond configuration (Figure 2a4) and O–H···N H-bond configuration (Figure 2b4,c4), respectively. However, methionine dimolecules are physically too large to form lateral hydrogen bonding within a half unit cell because of incompatibility of their size with respect to the separations of Si adatoms within a half unit cell.

For the simplest peptide, glycylglycine, with amino, amide, and carboxylic acid groups, our XPS result provides strong evidence for bidentate configuration, through either O–H and

N–H dissociation or double N–H dissociation, in the interfacial layer.³⁵ Formation of lateral H-bonds between two glycylglycine molecules adsorbed on the Si(111)7×7 surface in bidentate fashion is unlikely because of incompatible molecular dimensions with the separations between adjacent Si adatoms. Among all the configurations containing near-vertical H-bonds, our DFT-D2 results show that the configuration with the C=O···H–O hydrogen bonding is the most stable one in the transitional layer (Figure 2c5). Our calculated results are consistent with our XPS data, which indicate the absence of any O–H···N H-bond in the transitional layer.³⁵

These dimolecular structures have indeed been verified by STM. As examples, we show in Figure 2d1,d2, STM images of cysteine³³ and methionine⁵⁰ in their early growth stage on Si(111)7×7. STM data for the other proteinogenic biomolecules have also been reported.^{33,51,52} Evidently, the two bright protrusions marked by an oval in the upper image of Figure 2d1 corresponds to the flat cysteine dimolecular structure within a half unit cell (Figure 2a3), while that in the lower image of Figure 2d1 corresponds to the tilted dimolecular structure across the dimer wall (Figure 2b3). Similarly, the dark depression marked by an oval in the upper image of Figure 2d2 corresponds to the flat methionine dimolecular structure across the dimer wall (Figure 2a4), while the bright protrusions of the three-point star in the lower image of Figure 2d2 shows a novel methionine trimer structure within a half unit cell.⁵⁰

The stability of the flat dimolecular structures involving intralayer H-bonds of the benchmark proteinogenic biomolecules on the Si(111)7×7 surface follows the trend: [more negative adsorption energy] cysteine > methionine > alanine > glycine [less negative]. On the other hand, the corresponding stability trend for the near-vertical dimolecular structures involving interlayer H-bonds becomes: [more negative adsorption energy] glycylglycine > methionine > cysteine > alanine \approx glycine [less negative].

Because these proteinogenic biomolecules contain various moieties with a wide range of adsorption energy on the Si surface, the resulting interfacial layer and transitional layer offer a new opportunity of creating not just “permanent” but indeed “semi-permanent” biofunctionalization, respectively. We summarize a few general observations here to guide future application development, involving the growth processes of other amino acids and larger biological molecules and biofunctionalization of Si surface.

- (1) Most,^{33–36} if not all, aliphatic proteinogenic biomolecules follow the “universal” three-stage film growth process on Si(111)7×7.
- (2) The formation of intralayer H-bonds in the interfacial layer leads to a more stable configuration (flat configuration) than the formation of interlayer H-bonds in the transitional layer (lateral/near-vertical configurations), with the more parallel configuration with respect to the surface being more favorable than the tilted or more upright configurations.

Table 1. Binding Energies (in eV) of Fitted Peak Maxima for Various XPS Core-Level Features and Their Assignments for Three Growth Stages on Si(111)7×7 Surface for Glycine (G), D-Alanine (A), L-Cysteine (C), L-Methionine (M), and Glycylglycine (GG)^a

Core level	Assignment	Interfacial layer G: >250 °C A: >250 °C C: >285 °C M: >285 °C GG: >250 °C	Transitional layer G: 100-200 °C A: 100-200 °C C: 175-<285 °C M: 175-285 °C GG: 200-250 °C	Zwitterionic layer G: ~70 °C A: ~70 °C C: ~85 °C M: ~85 °C GG: ~100 °C
O 1s	-OH -C=O	532.5-533.0	532.2-533.0	
	-NH-C=O			532.7 ^{GG}
	-COO ⁻			531.8-531.9
N 1s	-NH-Si	398.6-399.1	398.7-399.1	
	-NH ₂ -NH-CO-	400.6 ^{GG}		
	O-H...N	401.0 ^C	401.0-401.1 ^{G,A,C,M}	
	-NH ₃ ⁺			401.7-402.2
C 1s	-CH ₂ -S-Si	284.7 ^C	284.5 ^C	
	-CH ₂ -SH	285.6 ^C	285.6 ^C	285.9-286.0 ^C
	CH ₃ -	285.3 ^A	285.3 ^A	285.3 ^A
	-CH ₂ -	285.285.1 ^M	285.2-285.4 ^M	285.4-285.5 ^M
	-CH ₂ -S-CH ₃	285.7-285.8 ^M	285.8-285.9 ^M	285.9 ^M
	-NH-C=O	288.1 ^{GG}	288.4-288.7 ^{GG}	288.9 ^{GG}
	-CH-NH-	286.3-286.9	286.5-286.9	
	-CH-NH ₃ ⁺			286.7-286.9
	-COOH	288.9-289.7	288.9-289.7	
-COO ⁻			288.7-289.0	
S 2s	-S-Si	227.4 ^C	227.4 ^C	
	-SH		228.4 ^C	228.4 ^C
	-CH ₂ -S-CH ₃	228.1 ^M	228.1 ^M	228.1 ^M

^aThe values apply to all five benchmark proteinogenic biomolecules unless the applications to specific biomolecules are indicated by superscripts. The thermal stability of the interfacial layer, transitional layer, or zwitterionic layer is indicated by the temperature at which layer depletion starts to occur (as shown in the top row).

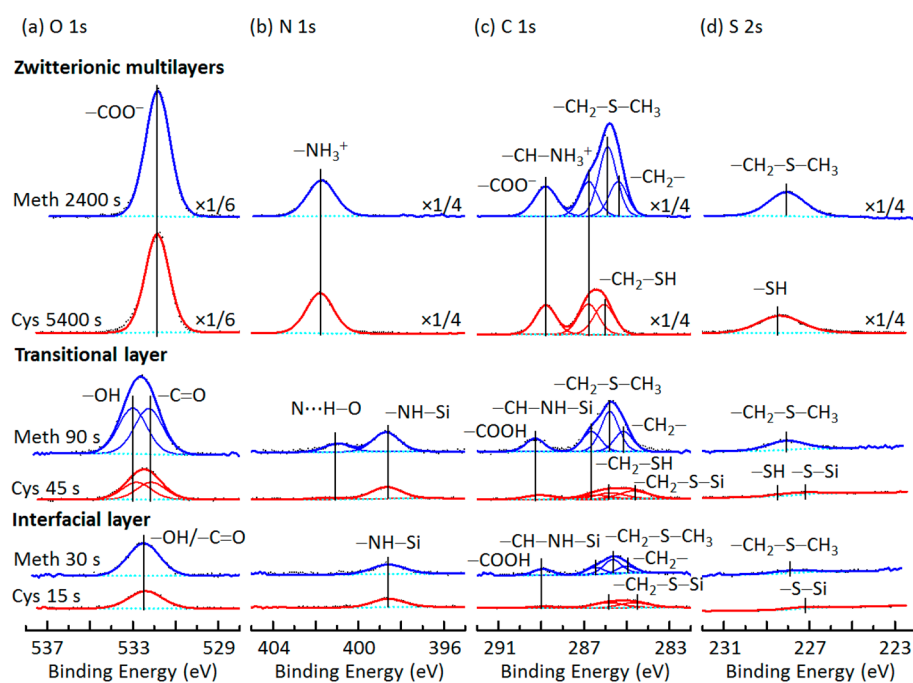


Figure 3. XPS spectra of the (a) O 1s, (b) N 1s, (c) C 1s, and (d) S 2s regions of L-methionine (Meth) and L-cysteine (Cys) deposited on Si(111)7×7 for three different exposure times that correspond to the interfacial layer, transitional layer, and zwitterionic multilayers. XPS data are fitted with individual components (solid line) corrected with a Shirley background (dotted line).

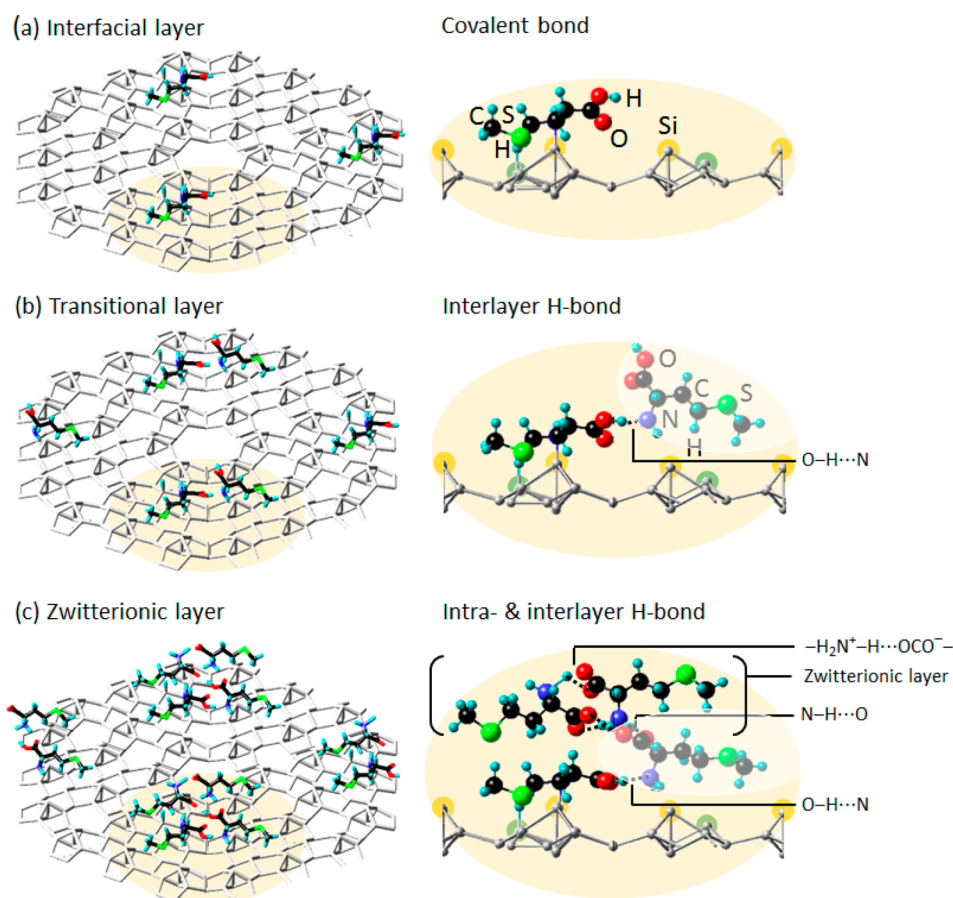


Figure 4. Three-stage growth model of L-methionine on Si(111)7×7 surface. Perspective views (left column) and magnified side views (right column) of (a) an interfacial layer, (b) a transitional layer, and (c) a zwitterionic layer. All equilibrium configurations are obtained by DFT-D2 calculations using a supercell of three 7×7 unit cells, each of which is represented by a Si₂₀₀H₄₉ slab, to model the 7×7 surface. Magnified side-views show (a) a methionine molecule adsorbed on a Si center adatom, (b) an interlayer N···H–O H-bond between molecules in the interfacial and transitional layers, and (c) additional interlayer O···H–N and O···H–O H-bonds between the transitional layer and zwitterionic layer and intralayer zwitterionic hydrogen bonding (O···H–N H-bond). For clarity, only the topmost layers of Si adatoms and the first bilayers of the three unit cells are shown. Si adatoms and restatoms are highlighted by larger yellow and green circles, respectively. The molecules in the transitional layer are slightly whitened for easier identification.

- (3) The interlayer O–H···N H-bond between a free carboxylic acid group in the interfacial layer and a free amino group in the transitional layer is found to be the most common mechanism in the early growth stage of these α -amino acids.
- (4) The formation of intralayer H-bonds between two adsorbed biomolecules in the interfacial layer depends on several factors: the size, nature, and available variety of the functional groups, conformer configuration, nature of possible adsorption sites on the surface, and steric hindrance among adsorbates and between an adsorbate and the surface registry.
- (5) In the case of interlayer H-bonds, not only do the orientations of both the first and second adsorbates play a crucial role on the adsorption energy, but also the site specificity of the Si surface could affect the viability of forming a stable dimolecule system.

■ “UNIVERSAL” THREE-STAGE GROWTH ON Si(111)7×7

To illustrate the importance of surface-mediated hydrogen bonding, we examine the “universal” three-stage growth found on the 7×7 surface for all the proteinogenic biomolecules

reported to date. Along with the results on the proteinogenic biomolecules shown in Table 1,^{33–36} XPS results for methionine (Supporting Information, section 4) also support a “universal” three-stage growth process on the 7×7 surface. As examples of (sulfur-containing) proteinogenic α -amino acids, we show in Figure 3 the O 1s, N 1s, C 1s, and S 2s spectra of methionine and cysteine for three different exposures exhibiting features corresponding to the interfacial layer, transitional layer, and zwitterionic multilayers. In Table 1, we summarize the XPS peak positions and their assignments for the interfacial layer, transitional layer, and zwitterionic multilayers in the five proteinogenic biomolecules adsorbed on the Si(111)7×7 surface. This reference table will provide an important guide to follow the adsorption of other amino acids and larger bioorganic molecules, such as proteins and peptides, on the reconstructed Si surface. For amino acids and peptides with only terminal amino and carboxylic acid groups, the biomolecule first forms covalent unidentate bonds to appropriate Si adatom sites through the dehydrogenated amino group, which builds up the interfacial layer. For the amino acid with an additional terminal functional group, such as thiol, the molecule can also form bidentate bonds to adjacent Si adatom sites at very low coverage. Further exposure produces

the transitional layer, the formation of which is driven by O–H···N H-bonds between a free carboxylic acid group in the first adlayer and a free amino group in the second adlayer. Finally, zwitterionic structures are obtained with continued exposure upon completion of the transitional layer.

In Figure 4, we summarize our large-scale DFT-D2 calculations for this universal three-stage growth process using methionine as an example. This process involves initial N–H dissociative adsorption followed by formation of an intermediate transitional layer involving O···H–N H-bonds, and the final formation of a zwitterionic multilayer film as a result of surface-mediated hydrogen bonding. In the interfacial layer, a methionine molecule binds with the dangling bond of a Si center adatom via a dehydrogenated amino group, which gives rise to a large variety of unidentate adsorption geometries on specific sites of the 7×7 surface, within a half unit cell and also across the dimer wall involving supplementary “weaker” long-range interactions of other functional groups (Supporting Information, section 2). The magnified side view of the interfacial layer (Figure 4a) shows a methionine molecule anchored to a Si adatom with a covalent –HN–Si bond, leaving the carboxylic acid (–COOH) group free to interact with a second methionine molecule. Our calculations suggest that the S lone-pair electrons could interact with other nearby Si adatoms or restatoms via weak long-range interactions. This is supported by our XPS results, which show no detectable change in the position of the S 2s peak over various methionine coverages (Supporting Information, section 4). Furthermore, the calculated equilibrium configuration of the transitional layer contains interlayer O–H···N H-bonds between the free carboxylic acid group of the first adsorbed methionine and a free amino group from a second methionine molecule (Figure 4b). This type of interlayer hydrogen bonding provides the driving force for the formation of the transitional layer. Finally, both intralayer and interlayer O···H–N H-bonds lead to the formation of a zwitterionic layer (Figure 4c).⁵³ Our DFT-D2 results demonstrate that intralayer interactions via O···H–N H-bonds or electrostatic forces between neighboring carboxylate (–COO[–]) and protonated amino (–NH₃⁺) groups lead to the formation of the zwitterionic layer. The zwitterionic layer is connected to the transitional layer through interlayer O···H–N hydrogen bonding between the carbonyl group (–C=O) of a free carboxylic acid group in the transitional layer and the –NH₃⁺ group in the zwitterionic layer and interlayer O–H···O hydrogen bonding between the hydroxyl group (–OH) of the carboxylic acid in the transitional layer and the –COO[–] group in the zwitterionic layer. As the result of these weak interactions, the zwitterionic layer is not as stable as the transitional layer and interfacial layer, which is confirmed by the thermal evolution of the corresponding XPS features (Table 1 and Supporting Information, section 4).

By consideration of the thermal stabilities of all five proteinogenic biomolecules in Table 1 (the first row), we also verify that the interfacial layer is more stable than the transitional layer, which is in turn more stable than the zwitterionic layer. Among the five proteinogenic biomolecules, the larger the biomolecule, the generally more stable is the individual layer. While the zwitterionic layer represents a less stable “temporary” adlayer and the interfacial layer corresponds to a very stable “permanent” adlayer, the transitional layers can be regarded as a “semi-permanent” one. The stabilities of these temporary, permanent, and semipermanent adlayers provide

the key to some interesting potential applications for biosensing and biofunctionalization applications.

Based on our XPS and DFT-D2 results, the aforementioned model is indeed applicable to all proteinogenic biomolecules on Si(111)7×7 surface reported to date. In Figure 5, a general

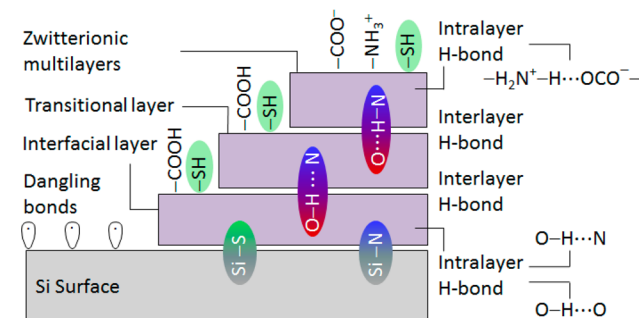


Figure 5. General schematic bonding model of available surface functional groups and all possible intralayer and interlayer interactions for the interfacial layer, transitional layer, and the zwitterionic multilayers of proteinogenic α -amino acids on Si(111)7×7 surface.

schematic bonding model shows available surface functional groups and possible intralayer and interlayer interactions for growth of the interfacial layer, transitional layer, and the zwitterionic multilayers. In addition to the intralayer O–H···O hydrogen bonding found in the interfacial layer for proteinogenic biomolecules with the amino and carboxylic acid groups, additional intralayer O–H···N hydrogen bonding in the interfacial layer is plausible for proteinogenic biomolecules with an additional functional group, such as thiol in cysteine, which enables additional anchoring options to the surface.

CONCLUSIONS

This Account demonstrates the importance of surface-mediated hydrogen bonding in the growth of proteinogenic biomolecules on a semiconductor surface. A “universal” three-stage growth process of five aliphatic proteinogenic biomolecules (i.e., glycine, alanine, cysteine, methionine, and glycyglycine) on Si(111)7×7 surface at room temperature have been observed using XPS.^{33–36} As supported also by large-scale DFT-D2 calculations, these benchmark biomolecules follow a similar binding pathway via N–Si bond formation in the interfacial layer. Our calculations also reveal that the formation of the transitional layer is driven by interlayer N···H–O hydrogen bonding between a free carboxylic acid and an amino group and is followed by the formation of a zwitterionic layer at higher exposure. The thermal stability of the zwitterionic layer is found to be lower than that of the transitional and interfacial layers because of the weaker intralayer and interlayer O···H–N H-bonds than the O–H···N H-bonds, as illustrated by DFT-D2 calculations for dimolecule systems in the gas phase or on the reconstructed Si surface. Such a growth model can be applied to larger biological molecules, such as peptides and proteins. We also establish the trends in the H-bond length among different types of hydrogen bonding for dimolecular structures in the gas phase (Figure 1) and on the Si(111)7×7 surface (Figure 2). Finally, five simple rules of thumb are developed to summarize the adsorption properties of these proteinogenic biomolecules as mediated by hydrogen bonding, and they are

expected to provide helpful guide to studies of larger biomolecules and their potential applications.

■ ASSOCIATED CONTENT

Supporting Information

The Supporting Information is available free of charge on the ACS Publications website at DOI: [10.1021/acs.accounts.5b00534](https://doi.org/10.1021/acs.accounts.5b00534).

DFT-D2 calculations for adsorption of five proteinogenic biomolecules on Si(111)7×7, single and dimolecular adsorption structures of methionine, dimolecular adsorption structures of cysteine, glycine, alanine, and glycyglycine, and nanofilm growth of methionine on Si(111)7×7 by X-ray photoelectron spectroscopy (PDF)

■ AUTHOR INFORMATION

Corresponding Author

*E-mail: tong@uwaterloo.ca.

Funding

This work was supported by the Natural Sciences and Engineering Research Council of Canada.

Notes

The authors declare no competing financial interest.

Biographies

Fatemeh R. Rahsepar received her B.Sc. in pure Chemistry and M.Sc. in Physical Chemistry from Isfahan University, and Ph.D. in Chemistry-Nanotechnology from the University of Waterloo. She is currently a postdoctoral research fellow at the University of Waterloo and is interested in biological surface chemistry, involving both experimental and computational studies for the development of bioelectronic devices.

Nafiseh Moghimi received her B.Sc. and M.Sc. in Physics from Shahid Beheshti University, and Ph.D. in Chemistry-Nanotechnology from the University of Waterloo. She is currently a postdoctoral research associate at WATLab, University of Waterloo, and she is working on design and development of hybrid nanomaterials for analytical and sensing applications.

Kam Tong Leung received his Ph.D. in Chemistry from the University of British Columbia. He is currently a Professor of Chemistry and the Director of the Waterloo Advanced Technology Laboratory (WATLab) at the University of Waterloo. His research interests include fundamental surface chemistry and materials science and their applications to catalysis, green energy, and chemical sensing.

■ REFERENCES

- (1) Hamers, R. J. Formation and Characterization of Organic Monolayers on Semiconductor Surfaces. *Annu. Rev. Anal. Chem.* **2008**, *1*, 707–736.
- (2) Mirkin, C. A.; Taton, T. A. Semiconductors Meet Biology. *Nature* **2000**, *405*, 626–627.
- (3) *Nanobiotechnology: Concepts, Applications and Perspectives*, 1st ed.; Niemeyer, C. M., Mirkin, C. A., Ed.; Wiley-VCH Verlag GmbH & Co. KGaA: Weinheim, Germany, 2004.
- (4) Tao, F.; Bernasek, S. L. *Functionalization of Semiconductor Surfaces*; Johan Wiley & Sons, Inc.: Hoboken, NJ, 2012.
- (5) Barlow, S. M.; Kitching, K. J.; Haq, S.; Richardson, N. V. A Study of Glycine Adsorption on a Cu{110} Surface Using Reflection Absorption Infrared Spectroscopy. *Surf. Sci.* **1998**, *401*, 322–335.
- (6) Lofgren, P.; Krozer, A.; Lausmaa, J.; Kasemo, B. Glycine on Pt (111): A TDS and XPS Study. *Surf. Sci.* **1997**, *370*, 277–292.

- (7) Zhao, X.; Rodriguez, J. Photoemission Study of Glycine Adsorption on Cu/Au(111) Interfaces. *Surf. Sci.* **2006**, *600*, 2113–2121.

- (8) Iwai, H.; Egawa, C. Molecular Orientation and Intermolecular Interaction in Alanine on Cu(001). *Langmuir* **2010**, *26*, 2294–2300.

- (9) Haq, S.; Massey, A.; Moslemzadeh, N.; Robin, A.; Barlow, S. M.; Raval, R. Racemic versus Enantiopure Alanine on Cu(110): An Experimental Study. *Langmuir* **2007**, *23*, 10694–10700.

- (10) Barlow, S. M.; Louafi, S.; Le Roux, D.; Williams, J.; Muryn, C.; Haq, S.; Raval, R. Supramolecular Assembly of Strongly Chemisorbed Size- and Shape-Defined Chiral Clusters: S- and R-Alanine on Cu(110). *Langmuir* **2004**, *20*, 7171–7176.

- (11) Barlow, S. M.; Louafi, S.; Le Roux, D.; Williams, J.; Muryn, C.; Haq, S.; Raval, R. Polymorphism in Supramolecular Chiral Structures of R- and S-Alanine on Cu(110). *Surf. Sci.* **2005**, *590*, 243–263.

- (12) Jones, G.; Jones, L. B.; Thibault-Starzyk, F.; Seddon, E. A.; Raval, R.; Jenkins, S. J.; Held, G. The Local Adsorption Geometry and Electronic Structure of Alanine on Cu{110}. *Surf. Sci.* **2006**, *600*, 1924–1935.

- (13) Madden, D. C.; Temprano, I.; Sacchi, M.; Blanco-Rey, M.; Jenkins, S. J.; Driver, S. M. Self-Organized Overlayers Formed by Alanine on Cu {311} Surfaces. *J. Phys. Chem. C* **2014**, *118*, 18589–18603.

- (14) Smerieri, M.; Vattuone, L.; Costa, D.; Tielens, F.; Savio, L. Self-Assembly of (S)-Glutamic Acid on Ag(100): A Combined LT-STM and Ab Initio Investigation. *Langmuir* **2010**, *26*, 7208–7215.

- (15) Smerieri, M.; Vattuone, L.; Kravchuk, T.; Costa, D.; Savio, L. (S)-Glutamic Acid on Ag(100): Self-Assembly in the Nonzwitterionic Form. *Langmuir* **2011**, *27*, 2393–2404.

- (16) Tranca, I.; Smerieri, M.; Savio, L.; Vattuone, L.; Costa, D.; Tielens, F. Unraveling the Self-Assembly of the (S)-Glutamic Acid “Flower” Structure on Ag(100). *Langmuir* **2013**, *29*, 7876–7884.

- (17) Jones, T. E.; Baddeley, C. J.; Gerbi, A.; Savio, L.; Rocca, M.; Vattuone, L. Molecular Ordering and Adsorbate Induced Faceting in the Ag {110}-(S)-Glutamic Acid System. *Langmuir* **2005**, *21*, 9468–9475.

- (18) Humblot, V.; Méthivier, C.; Pradier, C.-M. Adsorption of L-Lysine on Cu(110): A RAIRS Study from UHV to the Liquid Phase. *Langmuir* **2006**, *22*, 3089–3096.

- (19) Humblot, V.; Méthivier, C.; Raval, R.; Pradier, C.-M. Amino Acid and Peptides on Cu(110) Surfaces: Chemical and Structural Analyses of L-Lysine. *Surf. Sci.* **2007**, *601*, 4189–4194.

- (20) Zhao, X.; Zhao, R. G.; Yang, W. S. Scanning Tunneling Microscopy Investigation of L-Lysine Adsorbed on Cu(001). *Langmuir* **2000**, *16*, 9812–9818.

- (21) Uvdal, K.; Bodo, P.; Liedberg, B. L-Cysteine Adsorbed on Gold and Copper: An X-Ray Photoelectron Spectroscopy Study. *J. Colloid Interface Sci.* **1992**, *149*, 162–173.

- (22) Fischer, S.; Papageorgiou, A. C.; Marschall, M.; Reichert, J.; Diller, K.; Klappenberger, F.; Allegretti, F.; Nefedov, A.; Woll, C.; Barth, J. V. L-Cysteine on Ag(111): A Combined STM and X-Ray Spectroscopy Study of Anchorage and Deprotonation. *J. Phys. Chem. C* **2012**, *116*, 20356–20362.

- (23) Kühnle, A.; Linderoth, T. R.; Hammer, B.; Besenbacher, F. Chiral Recognition in Dimerization of Adsorbed Cysteine Observed by Scanning Tunneling Microscopy. *Nature* **2002**, *415*, 891–893.

- (24) Naitabdi, A.; Humblot, V. Chiral Self-Assemblies of Amino-Acid Molecules: D- and L-Methionine on Au(111) Surface. *Appl. Phys. Lett.* **2010**, *97*, 223112.

- (25) Schiffrin, A.; Riemann, A.; Auwarter, W.; Pennec, Y.; Weber-Bargioni, A.; Cvetko, D.; Cossaro, A.; Morgante, A.; Barth, J. V. Zwitterionic Self-Assembly of L-Methionine Nanogratings on the Ag(111) Surface. *Proc. Natl. Acad. Sci. U. S. A.* **2007**, *104*, 5279–5284.

- (26) Schiffrin, A.; Reichert, J.; Pennec, Y.; Auwarter, W.; Weber-Bargioni, A.; Marschall, M.; Dell’Angela, M.; Cvetko, D.; Bavdek, G.; Cossaro, A.; Morgante, A.; Barth, J. V. Self-Assembly of L-Methionine on Cu(111): Steering Chiral Organization by Substrate Reactivity and Thermal Activation. *J. Phys. Chem. C* **2009**, *113*, 12101–12108.

- (27) Humblot, V.; Tielens, F.; Luque, N. B.; Hampartsoumian, H.; Méthivier, C.; Pradier, C.-M. Characterization of Two-Dimensional Chiral Self-Assemblies L- and D-Methionine on Au(111). *Langmuir* **2014**, *30*, 203–212.
- (28) Méthivier, C.; Humblot, V.; Pradier, C.-M. L-Methionine Adsorption on Cu(110), Binding and Geometry of the Amino Acid as a Function of Coverage. *Surf. Sci.* **2015**, *632*, 88–92.
- (29) Wang, D.; Xu, Q.-M.; Wan, L.-J.; Bai, C.-L.; Jin, G. Adsorption of Enantiomeric and Racemic Tyrosine on Cu(111): A Scanning Tunneling Microscopy Study. *Langmuir* **2003**, *19*, 1958–1962.
- (30) Reichert, J.; Schiffrin, A.; Auwarter, W.; Weber-bargioni, A.; Marschall, M.; Dell'Angela, M.; Cvetko, D.; Bavdek, G.; Cossaro, A.; Morgante, A.; Barth, J. V. L-Tyrosine on Ag(111): Universality of the Amino Acid 2D Zwitterionic Bonding Scheme? *ACS Nano* **2010**, *4*, 1218–1226.
- (31) Forster, M.; Dyer, M. S.; Persson, M.; Raval, R. Probing Conformers and Adsorption Footprints at the Single-Molecule Level in a Highly Organized Amino Acid Assembly of (S)-Proline on Cu(110). *J. Am. Chem. Soc.* **2009**, *131*, 10173–10181.
- (32) Seljamae-Green, R. T.; Simpson, G. J.; Grillo, F.; Greenwood, J.; Francis, S. M.; Schaub, R.; Lacovig, P.; Baddeley, C. J. Assembly of a Chiral Amino Acid on an Unreactive Surface: (S)-Proline on Au(111). *Langmuir* **2014**, *30*, 3495–3501.
- (33) Rahsepar, F. R.; Zhang, L.; Farkhondeh, H.; Leung, K. T. Biofunctionalization of Si(111)7×7 by “Renewable” L-Cysteine Transitional Layer. *J. Am. Chem. Soc.* **2014**, *136*, 16909–16918.
- (34) Zhang, L.; Chatterjee, A.; Ebrahimi, M.; Leung, K. T. Hydrogen-Bond Mediated Transitional Adlayer of Glycine on Si(111)7×7 at Room Temperature. *J. Chem. Phys.* **2009**, *130*, 121103.
- (35) Zhang, L.; Chatterjee, A.; Leung, K. T. Three-Stage Growth of Glycine and Glycylglycine Nanofilms on Si(111)7×7 and Their Thermal Evolution in Ultrahigh Vacuum Condition: From Chemisorbed Adstructures to Transitional Adlayer to Zwitterionic Films. *J. Phys. Chem. C* **2011**, *115*, 14155–14163.
- (36) Zhang, L.; Chatterjee, A.; Leung, K. T. Hydrogen-Bond-Mediated Biomolecular Trapping: Reversible Catch-and-Release Process of Common Biomolecules on a Glycine-Functionalized Si(111)7×7 Surface. *J. Phys. Chem. Lett.* **2010**, *1*, 3385–3390.
- (37) Barth, J. V.; Weckesser, J.; Cai, C.; Günter, P.; Bürgi, L.; Jeandupeux, O.; Kern, K. Building Supramolecular Nanostructures at Surfaces by Hydrogen Bonding. *Angew. Chem., Int. Ed.* **2000**, *39*, 1230–1234.
- (38) Tao, F.; Bernasek, S. L. Understanding Odd–Even Effects in Organic Self-Assembled Monolayers. *Chem. Rev.* **2007**, *107*, 1408–1453.
- (39) Kühnle, A.; Linderth, T. R.; Besenbacher, F. Self-Assembly of Monodispersed, Chiral Nanoclusters of Cysteine on the Au(110)-(1 × 2) Surface. *J. Am. Chem. Soc.* **2003**, *125*, 14680–14681.
- (40) Grimme, S. Semiempirical GGA-Type Density Functional Constructed with a Long-Range Dispersion Correction. *J. Comput. Chem.* **2006**, *27*, 1787–1799.
- (41) Wang, Y.; Perdew, J. P. Correlation Hole of the Spin-Polarized Electron Gas, with Exact Small-Wave-Vector and High-Density Scaling. *Phys. Rev. B: Condens. Matter Mater. Phys.* **1991**, *44*, 13298–13307.
- (42) Perdew, J. P.; Chevary, J. A.; Vosko, S. H.; Jackson, K. A.; Pederson, M. R.; Singh, D. J.; Fiolhais, C. Atoms, Molecules, Solids, and Surfaces: Applications of the Generalized Gradient Approximation for Exchange and Correlation. *Phys. Rev. B: Condens. Matter Mater. Phys.* **1992**, *46*, 6671–6687.
- (43) Perdew, J. P.; Burke, K.; Ernzerhof, M. Generalized Gradient Approximation Made Simple. *Phys. Rev. Lett.* **1996**, *77*, 3865–3868.
- (44) Blochl, P. E. Projector Augmented-Wave Method. *Phys. Rev. B: Condens. Matter Mater. Phys.* **1994**, *50*, 17953–17979.
- (45) Kresse, G.; Joubert, D. From ultrasoft pseudopotentials to the projector augmented-wave method. *Phys. Rev. B: Condens. Matter Mater. Phys.* **1999**, *59*, 1758–1775.
- (46) Kresse, G.; Hafner, J. Ab Initio Molecular Dynamics for Liquid Metals. *Phys. Rev. B: Condens. Matter Mater. Phys.* **1993**, *47*, 558–561.
- (47) Kresse, G.; Hafner, J. Ab Initio Molecular-Dynamics Simulation of the Liquid-Metal—amorphous-Semiconductor Transition in Germanium. *Phys. Rev. B: Condens. Matter Mater. Phys.* **1994**, *49*, 14251–14269.
- (48) Kresse, G.; Furthmüller, J. Efficient Iterative Schemes for Ab Initio Total-Energy Calculations Using a Plane-Wave Basis Set. *Phys. Rev. B: Condens. Matter Mater. Phys.* **1996**, *54*, 11169–11186.
- (49) Kresse, G.; Furthmüller, J. Efficiency of Ab-Initio Total Energy Calculations for Metals and Semiconductors Using a Plane-Wave Basis Set. *Comput. Mater. Sci.* **1996**, *6*, 15–50.
- (50) Rahsepar, F. R. Surface Interactions of Proteinogenic Biomolecules and Gold Nanostructures on Si(111)7×7. Ph.D. Thesis, University of Waterloo, 2015.
- (51) Chatterjee, A.; Zhang, L.; Leung, K. T. Bidentate Surface Structures of Glycylglycine on Si(111)7×7 by High-Resolution Scanning Tunneling Microscopy: Site-Specific Adsorption via N–H and O–H or Double N–H Dissociation. *Langmuir* **2012**, *28*, 12502–12508.
- (52) Chatterjee, A.; Zhang, L.; Leung, K. T. Direct Imaging of Hydrogen Bond Formation in Dissociative Adsorption of Glycine on Si(111)7×7 by Scanning Tunneling Microscopy. *J. Phys. Chem. C* **2012**, *116*, 10968–10975.
- (53) Chen, Q.; Richardson, N. V. Enantiomeric Interactions between Nucleic Acid Bases and Amino Acids on Solid Surfaces. *Nat. Mater.* **2003**, *2*, 324–328.